AIP | The Journal of Chemical Physics

Structure and dynamics of water at the mackinawite (001) surface

Umberto Terranova and Nora H. de Leeuw

Citation: The Journal of Chemical Physics **144**, 094706 (2016); doi: 10.1063/1.4942755
View online: http://dx.doi.org/10.1063/1.4942755
View Table of Contents: http://scitation.aip.org/content/aip/journal/jcp/144/9?ver=pdfcov
Published by the AIP Publishing

Structure and dynamics of water at the mackinawite (001) surface

Umberto Terranova[1,2] and Nora H. de Leeuw[2,3]
[1]*Department of Chemistry, University College London, London WC1H 0AJ, United Kingdom*
[2]*School of Chemistry, Cardiff University, Cardiff CF10 3AT, United Kingdom*
[3]*Department of Earth Sciences, Utrecht University, 3584 CC Utrecht, The Netherlands*

(Received 22 December 2015; accepted 12 February 2016; published online 7 March 2016)

We present a molecular dynamics investigation of the properties of water at the interface with the mackinawite (001) surface. We find water in the first layer to be characterised by structural properties which are reminiscent of hydrophobic substrates, with the bulk behaviour being recovered beyond the second layer. In addition, we show that the mineral surface reduces the mobility of interfacial water compared to the bulk. Finally, we discuss the important differences introduced by simulating water under conditions of high temperature and pressure, a scenario relevant to geochemistry. © *2016 AIP Publishing LLC*. [http://dx.doi.org/10.1063/1.4942755]

I. INTRODUCTION

Iron-sulphide minerals in aqueous environment are of significant geochemical interest.[1,2] Not surprisingly, the interface between pyrite (FeS_2), the most common sulphide mineral on Earth, and water, has been widely investigated, both theoretically[3–7] and experimentally.[8,9]

Mackinawite (FeS) in aqueous systems has also attracted considerable attention, especially as an exceptional scavenger of heavy metals and radionuclides.[10] FeS has been shown to adsorb and reduce mercurium to its elemental state, thereby limiting the formation of toxic methylmercury in sediments.[11,12] Similarly, the catalytic reduction of soluble hexavalent uranium by FeS provides an effective method for remediation of contaminated groundwater.[13–15]

Recently, increasing interest has been concentrated on the role of mackinawite as a possible catalyst in the formation of primordial organic molecules at hydrothermal vents.[16,17] Indeed, experiments simulating chimney growth under early Earth conditions have revealed the presence of mackinawite,[18] while it has been demonstrated that FeS surfaces can activate carbon dioxide as a first step towards the formation of larger compounds.[19] FeS layers with intercalated water molecules have been suggested to provide reactive compartments.[20]

The adsorption of ions and molecules on mineral surfaces is affected by the structural and dynamical properties of interfacial water, with implications for potential applications of mackinawite.[21] However, despite its relevance, the interface between FeS and water has rarely been investigated,[20] and little is known how the mineral influences the properties of the interfacial water.

Here, we present a molecular dynamics (MD) investigation of water at the interface with the dominant mackinawite (001) surface. The emerging picture is that of a hydrophobic substrate which clearly affects the properties of nearby water. In addition, our findings show that both the structure and dynamics of water change dramatically when the extreme thermodynamic conditions, typical of hydrothermal vents, are taken into account.

II. METHODS

A. Interface models

Mackinawite consists of layers stacked along the *c*-axis, held together by Van der Waals forces.[22] Each layer is formed by FeS_4 edge-sharing tetrahedra arranged in a tetragonal lattice ($a = b = 3.67$ Å, $c = 5.03$ Å[23]), shown in Figure 1. Due to the lack of dangling bonds, the (001) surface is the most stable, and shows little relaxation compared to the bulk material.[24]

In order to model the interface, we have started from a $9 \times 9 \times 5$ supercell of mackinawite, containing 405 tetragonal Fe_2S_2 units. We have expanded the *c* vector of the supercell to 67 Å, creating a vacuum of around 40 Å to be subsequently filled with water molecules. After testing, we have found that the addition of 1523 water molecules into the cavity reproduces in the centre of the supercell the desired water density of 1.01 g cm^{-3},[25] which guarantees that molecules at the interface are in equilibrium with water under ambient conditions. The periodic simulation cell is illustrated in Figure 2.

To reproduce the interface at a typical hydrothermal vent condition (500 K, 400 atm), we have adjusted the total number of water molecules. We have performed preliminary tests and verified that 1296 water molecules mimic the corresponding tabulated water density (0.87 g cm^{-3} [26]) in the centre of the supercell.

B. Simulation details

MD simulations were carried out with DL_POLY_4,[27] using the force field introduced in Ref. 28, which we derived by refining, and consistently merging with the SPC/Fw model of water,[25] a set of existing interatomic potentials for the mineral.[24] In this force field, the mackinawite pairwise interactions can be written as a function of the interatomic distances r_{ij},

$$U_{ij} = A\exp\left(-\frac{r_{ij}}{\rho}\right) - \frac{C}{r_{ij}^6} + \frac{q_i q_j}{r_{ij}}, \quad (1)$$

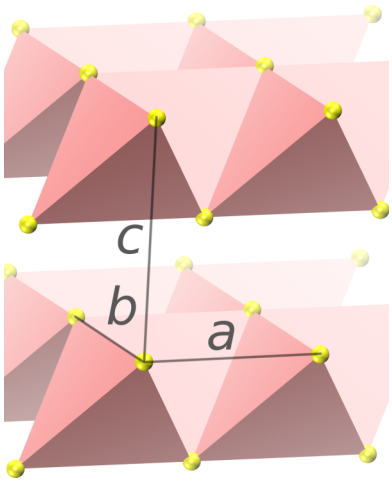

FIG. 1. Structure of mackinawite showing two layers formed by FeS_4 tetrahedra. Colour code: Fe (tetrahedra)—pink and S—yellow.

where A, ρ, and C are the coefficients of Buckingham potentials, and q_i the electrostatic charges of the atoms. To take into account polarisability effects, each sulfur atom is represented by a core and a massless shell interacting through a harmonic potential,

$$U_{ij} = \frac{1}{2} k_s r_{ij}^2, \tag{2}$$

where k_s is the shell force constant, and r_{ij} the core–shell distance. In addition, a three-body term acts between the S–Fe–S angles,

$$U_{ijk} = \frac{1}{2} k_{tb} (\theta_{ijk} - \theta_0)^2, \tag{3}$$

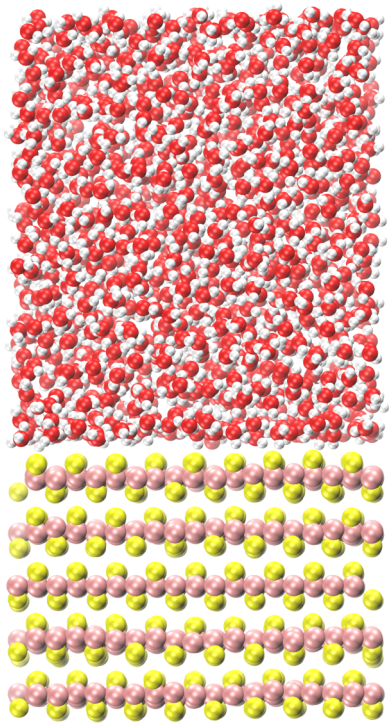

FIG. 2. Simulation cell employed for the mackinawite–water system. Colour code: Fe—pink, S—yellow, O—red, and H—white.

TABLE I. Force field parameters for mackinawite in an aqueous environment (from Ref. 28). Water molecules are described by the SPC/Fw model.[25]

Buckingham[a]	A (eV)	ρ (Å)	C (eV Å^6)
Fe–S_{shell}	1 000.00	0.3200	0.0
S_{shell}–S_{shell}	9 201.82	0.3147	130.0
Fe–O	48 294.40	0.160	0.00
S_{shell}–O	5 586.76	0.320	134.23
Lennard-Jones 12-10[a]	ε (eV)	σ (Å)	
S_{shell}–H	0.009 27	2.82	
Harmonic three-body[b]	θ_0 (deg)	k_{tb} (eV rad^{-2})	
S–Fe–S	109.47	3.0	
Harmonic shell	k_s (eV Å^{-2})		
S–S_{shell}	23.0		
Species	q (e)		
Fe	+2.000		
S	+1.357		
S_{shell}	−3.357		

[a]Cutoff: 9.0 Å.
[b]Cutoff: 3.0 Å.

where θ_0 is the tetrahedral S–Fe–S angle, and k_{tb} the associated force constant. The interaction potentials between water and mackinawite are given by

$$U_{ij} = A \exp\left(-\frac{r_{ij}}{\rho}\right) - \frac{C}{r_{ij}^6} + \varepsilon\left[5\left(\frac{\sigma}{r_{ij}}\right)^{12} - 6\left(\frac{\sigma}{r_{ij}}\right)^{10}\right] + \frac{q_i q_j}{r_{ij}}, \tag{4}$$

where ε and σ are, respectively, the strength and the equilibrium distance of the Lennard-Jones 12-10 potential. The force field parameters are listed in Table I. In Ref. 28, we have shown that they accurately reproduce density functional theory results of water adsorption on the low-index surfaces of mackinawite, and that the force field description of the behaviour of water intercalated into the FeS layers under extreme thermodynamic conditions is very similar to that found by *ab initio* MD.[20]

We have employed the NVT ensemble,[29] with a thermostat relaxation time of 0.1 ps. The MD simulations ran for 1 ns, and the data were collected during the last 0.5 ns of trajectory. The time step corresponded to 0.5 fs. The smoothed particle mesh Ewald method was used to calculate the long range electrostatics,[30] with a precision of 10^{-6}. The real space part of the electrostatics calculations and the van der Waals potentials had a cutoff of 9.0 Å. Following the adiabatic method proposed by Mitchell and Fincham,[31] shells were assigned a mass of 0.1 Da.

III. RESULTS

A. Density profiles

Figure 3 shows the O and H density profiles along the normal to the interface. Three distinct layers of water are

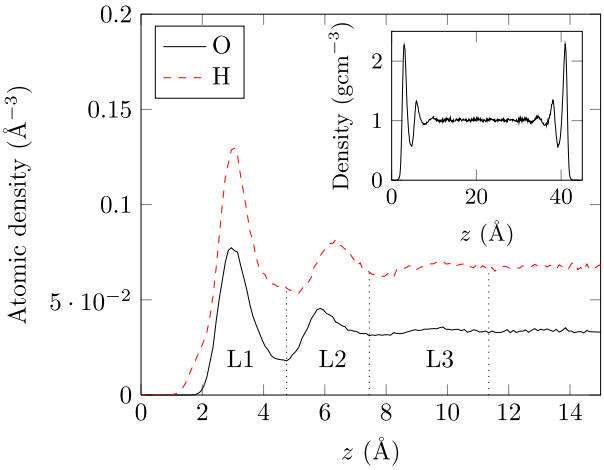

FIG. 3. Atomic density profiles as a function of the distance z from the mackinawite (001) surface. The inset shows the entire water density profile. The origin corresponds to the average position of the topmost S atoms. The dotted vertical lines, corresponding to the local minima of the O density profile, mark the three layers of water.

formed (L1, L2, L3), which can be assigned, respectively, to the O peaks at 2.95, 5.85, and 9.85 Å. The first H peak is at 3.05 Å, very close to the O peak in L1. Combined with the relative intensity between the two, it suggests the presence of a large fraction of molecules lying flat on the surface.

Overall, the O density profile is typical of a hydrophobic substrate. For example, graphene,[32] talc (001),[33] and pyrophyllite (001)[34,35] all share with mackinawite a thick region of depletion of water away from the surface, as well as similar separations between the peaks. One exception is the presence of a shoulder in the H atomic density, at around 1.8 Å, which we attribute to a small fraction of water molecules in L1 forming hydrogen bonds (HBs) with the surface.

B. Orientational and spatial ordering

In order to analyse the orientational ordering of water, we have introduced the angles β and ϕ, defined, respectively, as the angle between the normal to the plane of the water molecule and the surface normal (oriented towards the liquid phase), and between the OH vectors of water and the surface normal.

Figure 4 shows the probability distributions of $\cos\beta$ and $\cos\phi$ in the three layers. In L1, $\cos\beta$ has its most probable value at +1, i.e., evidence of a situation where the majority of water molecules stay flat in the proximity of the surface. Due to the geometry of a water molecule, in this configuration, both the OH vectors form an angle $\phi = 90°$. Molecules with this particular orientation, hereafter referred to as type Ia, are a hallmark of interfacial water on hydrophobic surfaces and follows from the necessity of maximising the number of HBs in the disrupted network at the interface.[36–38] In the L1 distribution of the angle between OH and the surface normal, a maximum at $\cos\phi = 1$ indicates a fraction of water molecules, which we will refer to as molecules of type Ib, with one OH vector aligned to the surface normal, and a second constrained at $\phi \approx 110°$. This contribution at $\cos\phi \approx -0.3$ mixes with the one at $\cos\phi = 0$ given by molecules of type Ia (for which

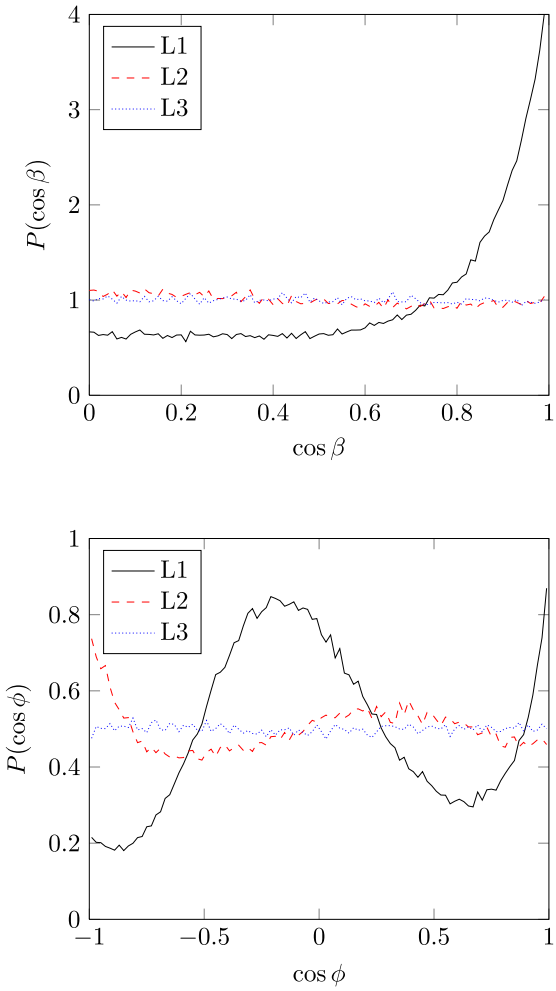

FIG. 4. Upper panel: probability density of the cosine of the angle β between the normal to the mackinawite (001) surface and the normal to the water molecular plane; lower panel: probability density of the cosine of the angle ϕ between the normal to the mackinawite (001) surface and the OH vector of water.

$\phi = 90°$), resulting into a single broad maximum centred in between the two. We note that the two preferential orientations in L1 coincide with those of water confined between graphene planes.[39] In L2, the $\cos\phi$ distribution shows two preferred orientations at $\phi \approx -1$ and $\phi \approx +0.4$, consistent with a single geometry where one OH vector is oppositely aligned to the interface normal. We will refer to these molecules as type II. We note that molecules in L3 have flat distributions, as we would expect for water molecules in the bulk. The angular ordering described above can be seen in a MD snapshot in Figure 5.

Beside characteristic orientations, water molecules in L1 of types Ia and Ib exhibit different propensities to reside on the surface. In order to visualise this, we show in Figure 6 their different surface distributions. While molecules of type Ib have no particular preferential location on the x–y plane, molecules of type Ia reside at the centre of squares whose vertices are the topmost S atoms. The presence of weak adsorption sites for water, reflecting the substrate geometry, is typical of hydrophobic clay minerals.[33,35] It is worth mentioning that we did not find any lateral order for molecules either in L2 or L3.

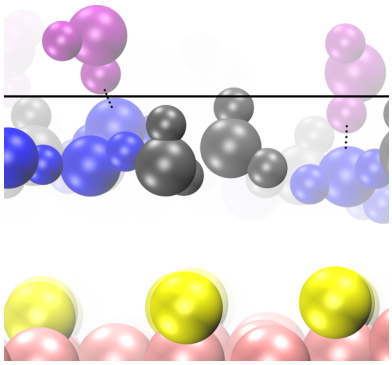

FIG. 5. Snapshot from the MD simulation. For clarity, we have shown only water molecules of the three types (Ia, Ib, II) described in the text. The thick line marks the boundary between L1 and L2, while the dotted lines are inter-layer HBs. Colour code: Fe—pink, S—yellow, type Ia water—blue, type Ib water—grey, and type II water—purple.

C. Hydrogen bond network

The ordering described in Subsection III B is closely connected to the HB network. As a criterion for water–water hydrogen-bonding, we have adopted a O–O distance smaller than 3.5 Å, and a O–H–O angle larger than 150°.[40] For water–surface hydrogen-bonding, we have adopted a O–S distance smaller than 3.7 Å, and a O–H–S angle larger than 140°.[41] If these criteria were satisfied, we assigned the bond to the mid-position between the donor and acceptor atoms.

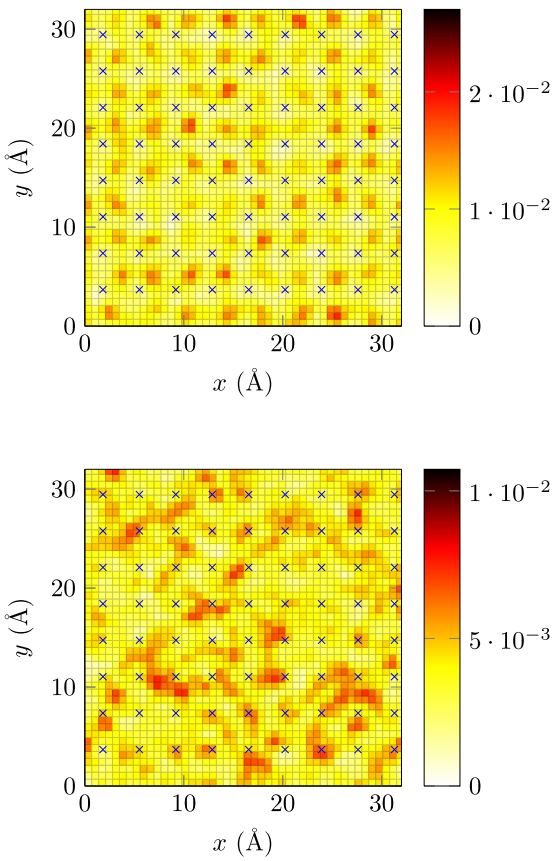

FIG. 6. Oxygen surface distributions (Å^{-3}) for type Ia (upper panel) and Ib (lower panel) water molecules in L1. Blue crosses mark the S atoms at the topmost plane of the mackinawite (001) surface. The grids have a resolution of 0.7 Å in each direction.

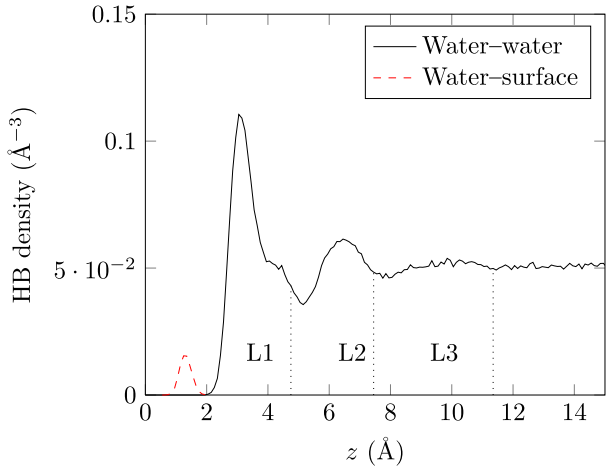

FIG. 7. HB density profile as a function of the distance z from the mackinawite (001) surface. The origin corresponds to the average position of the topmost S atoms.

Figure 7 shows the HB density profile as a function of the distance z from the surface. A peak at 3.05 Å, very close to the peak of the first layer in the density profile (2.95 Å), suggests the formation of a strong intra-layer HB network, while a minor peak at 6.45 Å can be attributed to the intra-layer network of the second water layer. In between, a shoulder marks the formation of inter-layer HBs, which is consistent with the picture of OH vectors of type Ib and II molecules pointing, respectively, towards and oppositely to the surface normal. As in the atomic density profiles (Figure 3), the third peak is almost indistinguishable, which reflects bulk behaviour of water. As shown by the ratio between the water–surface and the main intra-layer peak intensity, water molecules in L1 prefer to form HBs between themselves rather than anchoring to the surface.

Figure 8 depicts the distribution of the number of HBs per water molecule in the three layers. For comparison, we also plot results for a fourth region (B) centred at 22 Å from the surface, and with a thickness of 4 Å. The distributions in L2 and L3 coincide with that in B, and the average number of HBs per molecule, n_{HB}, is around 3.0 in the three regions (Table II). In contrast, the distribution in L1 is different. Here, although the most probable HB value remains three, the fraction of water molecules forming two HBs is larger than that forming four, which reverses the scenario described above. As a consequence, the average of the distribution drops to 2.75 HBs per molecule. We emphasise that, in L1, the fraction of HBs formed with the surface contributes only to a minor extent to the total fraction of HBs in the network, as clearly confirmed by Figure 8. Quantitatively, we find that only around 10% of the S atoms of the topmost plane accept on average HBs from water molecules.

D. Residence time

In order to estimate the residence time of water in the three layers (L1, L2, L3), we have calculated the residence

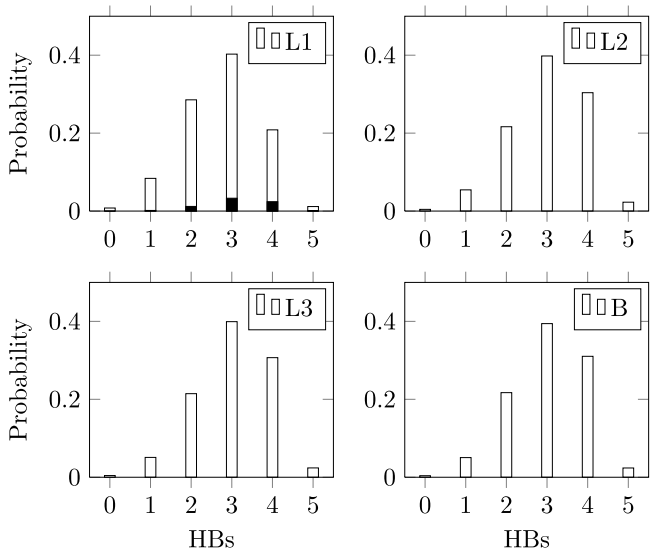

FIG. 8. Distributions of the number of HBs per water molecule formed in each region. In L1, the filled areas represent the contributions provided by the water–surface HBs.

correlation function of water,[42]

$$R(t) = \frac{\langle \theta(t_0 + t)\theta(t_0)\rangle}{\langle \theta(t_0)\theta(t_0)\rangle}, \quad (5)$$

where the brackets indicate an average over water molecules and time origins t_0, while the Heaviside step function $\theta(t_0 + t)$ equals 1 if a water molecule has never left the layer of interest in the time interval $[t_0,\ t_0 + t]$, and 0 otherwise. This definition corresponds to a continuous residence correlation function, as water molecules which temporarily leave their initial layer do not contribute to the statistics anymore.

In Figure 9, we plot $R(t)$ in the three layers. It can be noted that water molecules remain confined longer in L1 than in the other layers. A longer permanence of water has been reported also in the first layer of graphene, where the residence time τ_R, defined as the time required for $R(t)$ to decay to $1/e$ was of the order of tens of ps.[32,43] On the (001) surface of mackinawite, τ_R corresponds to 22.0 ps in L1 and drops to 5.5 and 6.5 ps, respectively, in L2 and L3. In order to be able to make a comparison with the behaviour of water in the bulk, we have calculated $R(t)$ also in the region B defined in Subsection III C, and subsequently normalised all τ_R by the thickness of the layers (4.75, 2.70, 3.90, and 4.00 Å for L1, L2, L3, and B, respectively).[44] The resulting τ'_R, listed in Table II, are independent of the extension of the regions along the surface normal and suggest strong surface effects

TABLE II. Average number of HBs per molecule (n_{HB}), residence time (τ_{R}), normalised residence time (τ'_{R}), and in-plane self-diffusion coefficient (D_{xy}) of water at the interface with the mackinawite (001) surface.

	n_{HB}	τ_{R} (ps)	τ'_{R} (ps Å^{-1})	D_{xy} (10^{-5} cm^2 s^{-1})
L1	2.75	22.0	4.63	1.97
L2	3.01	5.0	2.04	2.30
L3	3.03	6.5	1.79	2.43
B	3.03	6.5	1.62	2.58

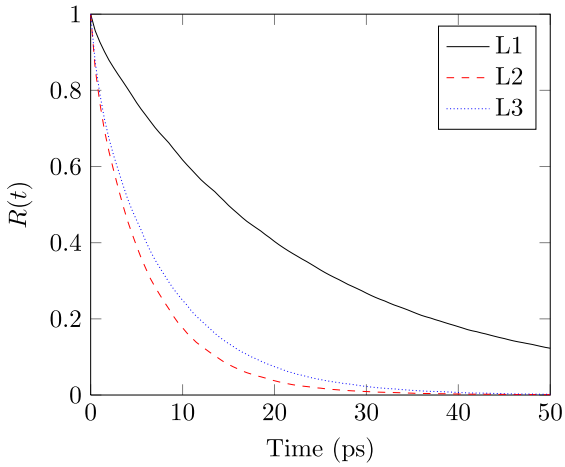

FIG. 9. Residence correlation functions of water in the three layers of the mackinawite (001) surface.

in L1. The impact of the surface is much weaker, but still appreciable, in L2 and L3.

E. Translational dynamics

Having demonstrated that the presence of the surface causes water molecules to stay longer in L1, we have investigated how the underlying mineral affects the diffusion of water. To this end, we have calculated the in-plane mean square displacement of the water oxygens belonging to a given region,

$$\mathrm{MSD}_{xy}(t) = \left\langle \big(x(t + t_0) - x(t_0)\big)^2 + \big(y(t + t_0) - y(t_0)\big)^2 \right\rangle, \quad (6)$$

where the average is over both time origins t_0 and water molecules remaining continuously in a given layer in the time interval $[t_0,\ t_0 + t]$. Once a molecule is not detected in that layer, it does not contribute to the calculation of MSD_{xy} anymore.

We present the results in Figure 10. Water molecules in all the layers of the mackinawite interface are slowed down compared to the bulk, but the effect is particularly strong in

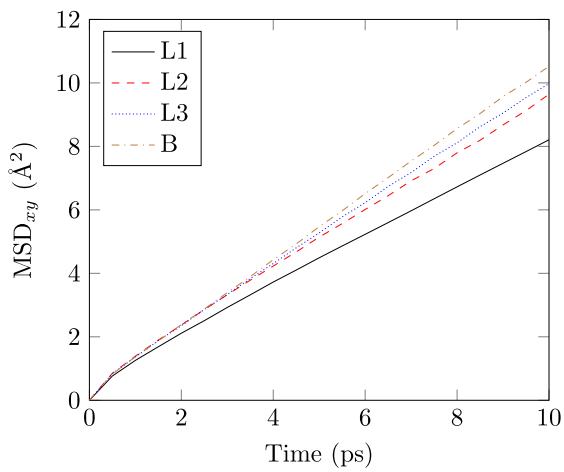

FIG. 10. Mean square displacements of water in the four regions of the mackinawite (001) surface.

L1. By fitting the MSD_{xy} curves to straight lines, it is possible to obtain a rough estimate of the self-diffusion coefficients in the x–y plane, defined by the Einstein relation,

$$D_{xy} = \lim_{t\to\infty} \frac{\mathrm{MSD}_{xy}(t)}{4t}. \quad (7)$$

An exact evaluation of D_{xy} would require accurate statistics at very long times, which, due to the short residence time of water in the layers, we are not able to obtain. Consequently, our value of D_{xy} in B (2.58×10^{-5} cm^2 s^{-1}) slightly differs from the expected value for three dimensional SPC/Fw bulk water (2.32×10^{-5} cm^2 s^{-1} [25]). However, in this analysis, we are more concerned with the comparison of D_{xy} between the regions, and not with determining its exact value.

As shown in Table II, the self-diffusion coefficient in L1 is reduced by ≈24% compared to the value in B. Interestingly, the diffusion of water is affected by the mineral even in layers as far as L3, where a 6% discrepancy with the coefficient in B remains. The reduction in mobility parallels the increase in residence times of water within the layers and is in line with the dynamical behaviour described at hydrophobic crystalline materials[45] and graphite–CH_3 plates.[46]

IV. EXTREME CONDITIONS

Finally, we have considered the behaviour of interfacial water at the conditions typical of hydrothermal vents (500 K, 400 atm), where mackinawite has been postulated to catalyse the formation of primordial organic compounds. We stress that *ab initio* MD simulations of water intercalated between mackinawite sheets under very similar thermodynamic conditions have not captured any surface reactivity,[20] validating the use of a classical approach to investigate the interface.

In Figure 11, we compare the density profiles of water under ambient and extreme conditions. In terms of peak positions and depletion regions, the differences between the two are negligible. However, we note the disappearance of the third layer of water, together with a reduction of the

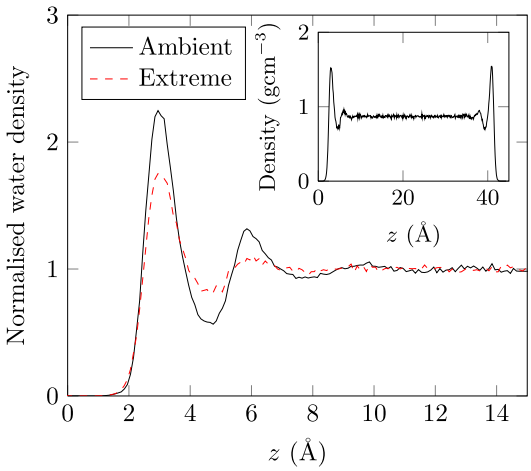

FIG. 11. Water density profiles as a function of the distance z from the mackinawite (001) surface (normalised to the bulk values in the centre of the supercell). The inset shows the entire profile at extreme conditions. The origin corresponds to the average position of the topmost S atoms.

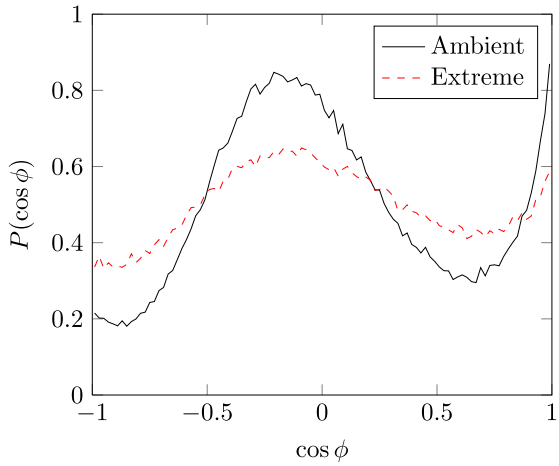

FIG. 12. Probability densities of the cosine of the angle ϕ between the normal to the mackinawite (001) surface and the OH vector of water.

TABLE III. Average number of HBs per molecule (n_{HB}), residence time (τ_{R}), normalised residence time (τ'_{R}), and in-plane self-diffusion coefficient (D_{xy}) of water at the interface with the mackinawite (001) surface under extreme conditions.

	n_{HB}	τ_{R} (ps)	τ'_{R} (ps Å^{-1})	D_{xy} (10^{-5} cm^2 s^{-1})
L1	1.74	3.5	0.75	17.65
L2	1.92	1.5	0.47	18.40
B	1.91	2.0	0.50	19.30

intensities of the peaks with respect to the bulk value. Figure 12 displays the distributions of $\cos\phi$ in L1. As indicated by a smoother curve, the fraction of water molecules of both types Ia and Ib is smaller under extreme conditions, suggesting less orientational ordering. The analysis of the HB network reveals that around 20% of the HBs in each layer are lost (Table III). This effect has also been observed for water confined in graphene nanochannels[39] and is consistent with the tendency of water to appear less structured.

The most significant differences arise when dynamical properties are investigated. Table III shows that under extreme conditions all the residence times diminish, while the self-diffusion coefficients increase by an order of magnitude, as expected from the diffusion behaviour of bulk water.[47] These results are in line with the faster desorption rate of water reported on graphene.[39] Similar to ambient conditions, water is slowed down at the interface compared to the bulk, but the bulk behaviour is approached at distances from the substrate as close as 5 Å.

V. CONCLUSIONS

We have performed MD simulations to characterise the structure and dynamics of water in contact with the most stable (001) surface of mackinawite. We find the behaviour of water to be consistent with that determined by a hydrophobic substrate. Accordingly, instead of hydrogen-bonding to the surface, water molecules in the first layer show an unambiguous tendency to form intra-layer HBs. The

ordering induced by the mineral, lost beyond distances of ≈8 Å, is accompanied by a slower diffusion of interfacial water molecules compared to the bulk.

When moving to extreme thermodynamic conditions of high temperature and pressure, the structural and orientational ordering of water reduces substantially, while the HB network is severely disrupted, as found by *ab initio* MD of supercritical water on pyrite.[48] However, it is in the dynamical behaviour that the most important differences manifest themselves, with self-diffusion coefficients increased by an order of magnitude.

The hydrophobic nature of mackinawite, especially under the conditions typically encountered in the deep ocean, seems to exclude the possibility of intercalation of water molecules between expanded FeS layers. However, it thus highlights the importance of also investigating edge surfaces exposing undercoordinated Fe_3S and FeS groups,[49] which we intend to examine in future work.

ACKNOWLEDGMENTS

This work was supported by the Natural Environment Research Council (Grant No. NE/J010626/1). The authors acknowledge the use of the UCL Legion High Performance Computing Facility (Legion@UCL), and associated support services, in the completion of this work. NHdL thanks the Royal Society for an Industry Fellowship.

[1]J. M. Guevremont, J. Bebie, A. R. Elsetinow, D. R. Strongin, and M. A. Schoonen, Environ. Sci. Technol. **32**, 3743–3748 (1998).
[2]M. Descostes, P. Vitorge, and C. Beaucaire, Geochim. Cosmochim. Acta **68**, 4559–4569 (2004).
[3]N. H. De Leeuw, S. C. Parker, H. M. Sithole, and P. E. Ngoepe, J. Phys. Chem. B **104**, 7969–7976 (2000).
[4]A. Stirling, M. Bernasconi, and M. Parrinello, J. Chem. Phys. **118**, 8917–8926 (2003).
[5]M. R. Philpott, I. Y. Goliney, and T. T. Lin, J. Chem. Phys. **120**, 1943–1950 (2004).
[6]P. H.-L. Sit, M. H. Cohen, and A. Selloni, J. Phys. Chem. Lett. **3**, 2409–2414 (2012).
[7]J. Chen, X. Long, and Y. Chen, J. Phys. Chem. C **118**, 11657–11665 (2014).
[8]S. Knipe, J. Mycroft, A. Pratt, H. Nesbitt, and G. Bancroff, Geochim. Cosmochim. Acta **59**, 1079–1090 (1995).
[9]H. Nesbitt and I. Muir, Geochim. Cosmochim. Acta **58**, 4667–4679 (1994).
[10]Y. Gong, J. Tang, and D. Zhao, Water Res. **89**, 309–320 (2016).
[11]S. E. Bone, J. R. Bargar, and G. Sposito, Environ. Sci. Technol. **48**, 10681–10689 (2014).
[12]H. Y. Jeong, B. Klaue, J. D. Blum, and K. F. Hayes, Environ. Sci. Technol. **41**, 7699–7705 (2007).
[13]L. N. Moyes, R. H. Parkman, J. M. Charnock, D. J. Vaughan, F. R. Livens, C. R. Hughes, and A. Braithwaite, Environ. Sci. Technol. **34**, 1062–1068 (2000).
[14]S. P. Hyun, J. A. Davis, K. Sun, and K. F. Hayes, Environ. Sci. Technol. **46**, 3369–3376 (2012).
[15]S. Y. Lee, M. H. Baik, H.-R. Cho, E. C. Jung, J. T. Jeong, J. W. Choi, Y. B. Lee, and Y. J. Lee, J. Radioanal. Nucl. Chem. **296**, 1311–1319 (2013).
[16]W. Martin and M. J. Russell, Philos. Trans. R. Soc., B **358**, 59–85 (2003).
[17]R. E. Mielke, K. J. Robinson, L. M. White, S. E. McGlynn, K. McEachern, R. Bhartia, I. Kanik, and M. J. Russell, Astrobiology **11**, 933–950 (2011).
[18]L. M. White, R. Bhartia, G. D. Stucky, I. Kanik, and M. J. Russell, Earth Planet. Sci. Lett. **430**, 105–114 (2015).
[19]N. Y. Dzade, A. Roldan, and N. H. de Leeuw, J. Chem. Phys. **143**, 094703 (2015).
[20]C. Wittekindt and D. Marx, J. Chem. Phys. **137**, 054710 (2012).
[21]G. E. Brown, Jr., Science **294**, 67 (2001).
[22]H. Ohfuji and D. Rickard, Earth Planet. Sci. Lett. **241**, 227–233 (2006).
[23]A. R. Lennie, S. Redfern, P. Schofield, and D. Vaughan, Mineral. Mag. **59**, 677–684 (1995).
[24]A. J. Devey, R. Grau-Crespo, and N. H. De Leeuw, J. Phys. Chem. C **112**, 10960–10967 (2008).
[25]Y. Wu, H. L. Tepper, and G. A. Voth, J. Chem. Phys. **124**, 024503 (2006).
[26]W. T. Holser and G. C. Kennedy, Am. J. Sci. **256**, 744–754 (1958).
[27]I. T. Todorov, W. Smith, K. Trachenko, and M. T. Dove, J. Mater. Chem. **16**, 1911–1918 (2006).
[28]U. Terranova and N. H. de Leeuw, Theor. Chem. Acc. **135**, 46 (2016).
[29]W. G. Hoover, Phys. Rev. A **31**, 1695 (1985).
[30]U. Essmann, L. Perera, M. L. Berkowitz, T. Darden, H. Lee, and L. G. Pedersen, J. Chem. Phys. **103**, 8577–8593 (1995).
[31]P. Mitchell and D. Fincham, J. Phys.: Condens. Matter **5**, 1031 (1993).
[32]D. Argyris, N. R. Tummala, A. Striolo, and D. R. Cole, J. Phys. Chem. C **112**, 13587–13599 (2008).
[33]J. Wang, A. G. Kalinichev, and R. J. Kirkpatrick, Geochim. Cosmochim. Acta **70**, 562–582 (2006).
[34]T. R. Zeitler, J. A. Greathouse, and R. T. Cygan, Phys. Chem. Chem. Phys. **14**, 1728–1734 (2012).
[35]G. Jeanmairet, V. Marry, M. Levesque, B. Rotenberg, and D. Borgis, Mol. Phys. **112**, 1320–1329 (2014).
[36]J. R. Grigera, S. G. Kalko, and J. Fischbarg, Langmuir **12**, 154–158 (1996).
[37]F. Sedlmeier, J. Janecek, C. Sendner, L. Bocquet, R. R. Netz, and D. Horinek, Biointerphases **3**, FC23–FC39 (2008).
[38]C.-Y. Lee, J. A. McCammon, and P. Rossky, J. Chem. Phys. **80**, 4448–4455 (1984).
[39]G. Nagy, M. Gordillo, E. Guàrdia, and J. Martí, J. Phys. Chem. B **111**, 12524–12530 (2007).
[40]A. Luzar and D. Chandler, Phys. Rev. Lett. **76**, 928 (1996).
[41]U. Terranova and N. H. de Leeuw, Phys. Chem. Chem. Phys. **16**, 13426–13433 (2014).
[42]R. Impey, P. Madden, and I. McDonald, J. Phys. Chem. A **87**, 5071–5083 (1983).
[43]T. A. Ho and A. Striolo, Mol. Simul. **40**, 1190–1200 (2014).
[44]J. Marti, G. Nagy, M. Gordillo, and E. Guardia, J. Chem. Phys. **124**, 094703 (2006).
[45]M. Ø. Jensen, O. G. Mouritsen, and G. H. Peters, J. Chem. Phys. **120**, 9729–9744 (2004).
[46]J. Li, T. Liu, X. Li, L. Ye, H. Chen, H. Fang, Z. Wu, and R. Zhou, J. Phys. Chem. B **109**, 13639–13648 (2005).
[47]K. Krynicki, C. D. Green, and D. W. Sawyer, Faraday Discuss. Chem. Soc. **66**, 199–208 (1978).
[48]A. Stirling, T. Rozgonyi, M. Krack, and M. Bernasconi, Phys. Chem. Chem. Phys. **17**, 17375–17379 (2015).
[49]M. Wolthers, L. Charlet, P. R. van Der Linde, D. Rickard, and C. H. van Der Weijden, Geochim. Cosmochim. Acta **69**, 3469–3481 (2005).